Supplementary Information (SI) for Journal of Materials Chemistry A.

Unveiling high-yield dinitrogen-to-green ammonia production *via* highly defective $Cu_4Bi_5S_{10}/Mn_4V_2O_9$ electrocatalysts performed in alkaline H-cell and stack-cell reactors

Merga Hailemariam Urgesa[1,4], Quoc-Nam Ha[1], Kuo-Hsin Lin[2], Li Duan Tsai[2], Yin-Wen Tsai[2] Dong-Hau Kuo[1,3*]

[1]Department of Material Science and Engineering, National Taiwan University of Science and Technology, Taipei 10607, Taiwan

[2]Material and Chemical Research Laboratories, Industrial Technology Research Institute, Chutung, Hsinchu 31040, Taiwan

[3]Graduate Institute of Energy and Sustainability Technology, National Taiwan University of Science and Technology, Taipei 10607, Taiwan

[4]Department of Chemistry, College of Natural and Computational Sciences, Ambo University, Ambo, Ethiopia

*Corresponding author

Fax: +001-886-2-27303291. E-mail: dhkuo@mail.ntust.edu.tw

Indophenol Blue and Nessler's reagent methods to determine ammonia concentration

Two methods were employed to determine ammonia (NH_3) concentration during the electrochemical nitrogen reduction reaction (IRR). Initially, in the Indophenol Blue method, 1.5 mL of the electrolyte for the N_2 reduction reaction sample was mixed with 2 mL of Solution A (1 M NaOH containing 5 wt.% sodium citrate and 5 wt.% salicylic acid), 1 mL of Solution B (0.05 M sodium hypochlorite), and 0.2 mL of solution C (1 wt.% sodium nitroprusside). Following a 1-30-min incubation in darkness, absorption spectra were measured between 500 and 800 nm using a UV–vis spectrophotometer, having the Indophenol Blue formation assessed at 655 nm. Standard concentration-absorbance curves were plotted using reference solutions of varying NH_4Cl concentrations dissolved in 0.5 M Na_2SO_4, with ammonia calculated by subtracting the absorbance of the background solution from the measured peaks of the N_2 reduction experiments. In Nessler's reagent method, 3 mL of sample was taken every 30 min, and the UV-visible absorption spectrum was measured in yellow-orange color. Calibration curves were created using a standard NH_4Cl solution with various concentrations, and NH_3 yield and percentage of Faradaic efficiency (FE) were calculated using the specified equations below. Furthermore, the potential by-product N_2H_4 is detected using the Watt and Chris method involving H_2SO_4 with $KMnO_4$.

Table S1 Molar content of each precursor chemical for preparing the electrochemical catalysts

No	Catalyst code	V(Ac) mmol	$Cu(NO_3)_2$ mmol	$Mn(NO_3)_2.4H_2O$ mmol	$Bi(NO_3)_3.5H_2O$ mmol	Product mass (mg)	Foam size (cm^2)
1	CuMn(2:3)	0	2	3	0	2.38	1:1
2	CuMn(3:1)	0	3	3	0	2.39	1:1
3	CuMn(3:2)	0	3	2	0	2.47	1:1
4	CuMnBi(3:2:2)	0	3	2	2	2.51	1:1
5	VCuMnBi(1:3:2:2)	1	3	2	2	2.62	1:1
6	VCuMnBi(2:3:2:2)	2	3	2	2	2.61	1:1
7	VCuMnBi(3:3:2:2)	3	3	2	2	2.67	1:1

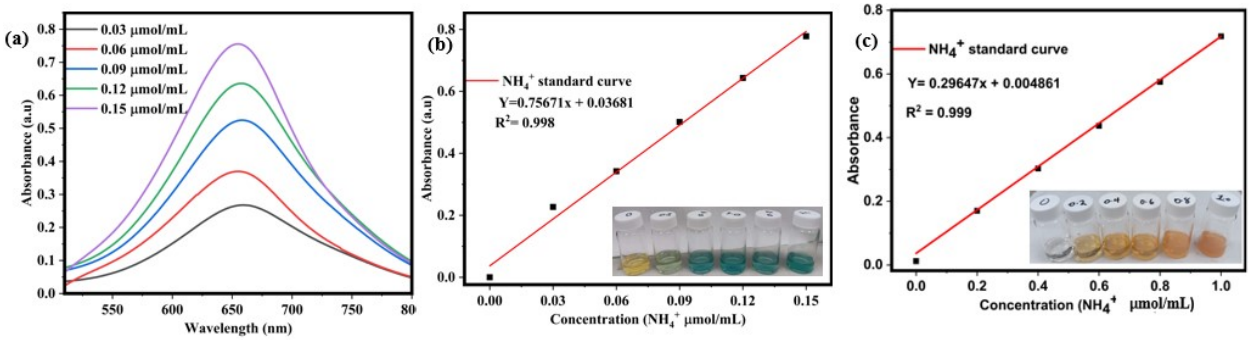

Fig. S1. (a) UV-Vis absorption spectra, (b) calibration curves for testing the colorimetric NH_3 assay employing the indophenol blue method, and (c) the calibration curve for testing with the Nessler's reagent.

The concentration of ammonia is calculated as below:

$$NH_3 \text{ yield} = \frac{C_{NH3} \times V}{t \times A} \quad \text{.....eq.1}$$

From the standard curve

Y=0.75671x + 0.03681

C_{NH3}(X)=((Y-0.03681)/0.75671)*17 g/mol

Due to the absorption of each ammonia product having a value greater than one, we have implemented dilution factors exceeding unity for each absorption.

Form question 1, NH_3 yield= $\left(\frac{C_{NH3} \times V}{t \times A}\right) * DF$

where C_{NH3} (μg/mL) is the measured NH_3 concentration, V(mL) is the volume of the electrolyte, t(h) is the reduction time, A(cm^2) is the area of nickel foam used, or m (mg) is the mass loading of the catalyst on the Ni foam used, and DF is the dilution factor.

Energy efficiency and energy consumption calculation

To compare the energy consumption of NH_3 electrosynthesis with that of the Haber-Bosch process, the related specific energy consumptions (EC) (KWh/kg) were calculated based on the following equation:

$$EC = \frac{n \times F \times V_{cell}}{3600 \times FE \times M} = \frac{3 \times 96485 \times 1.9}{3600 \times 0.372 \times 17} = 24.2\ kWh/kg_{NH3}$$

In the given equation, where n represents the number of transferred electrons per mole of product, F is the Faraday constant (C/mol), V_{cell} stands for the cell voltage (V), FE denotes the Faradaic efficiency, and M is the molar mass of the products, our work chose an optimized applied cell potential of 1.9 V to compute the energy consumption of ammonia synthesis to maximize the NH_3 yield rate.

The electrocatalytic energy efficiency (EE) of our single stack cell was calculated according to the below equation:

EE (%) =

$$\frac{1000 \times FE \times 339.2}{3 \times F \times (1.23 - \eta)} \times 100\% = \frac{1000 \times 0.372 \times 339.2}{3 \times 96485 \times (1.23 - 0.292)} \times 100\% = 46.5\%$$

η: overpotential, defined as the difference between the thermodynamic potential of NRR (E^o= 0.092 V vs. RHE) and the applied potential to initiate the eNRR (-0.2 V vs. RHE))

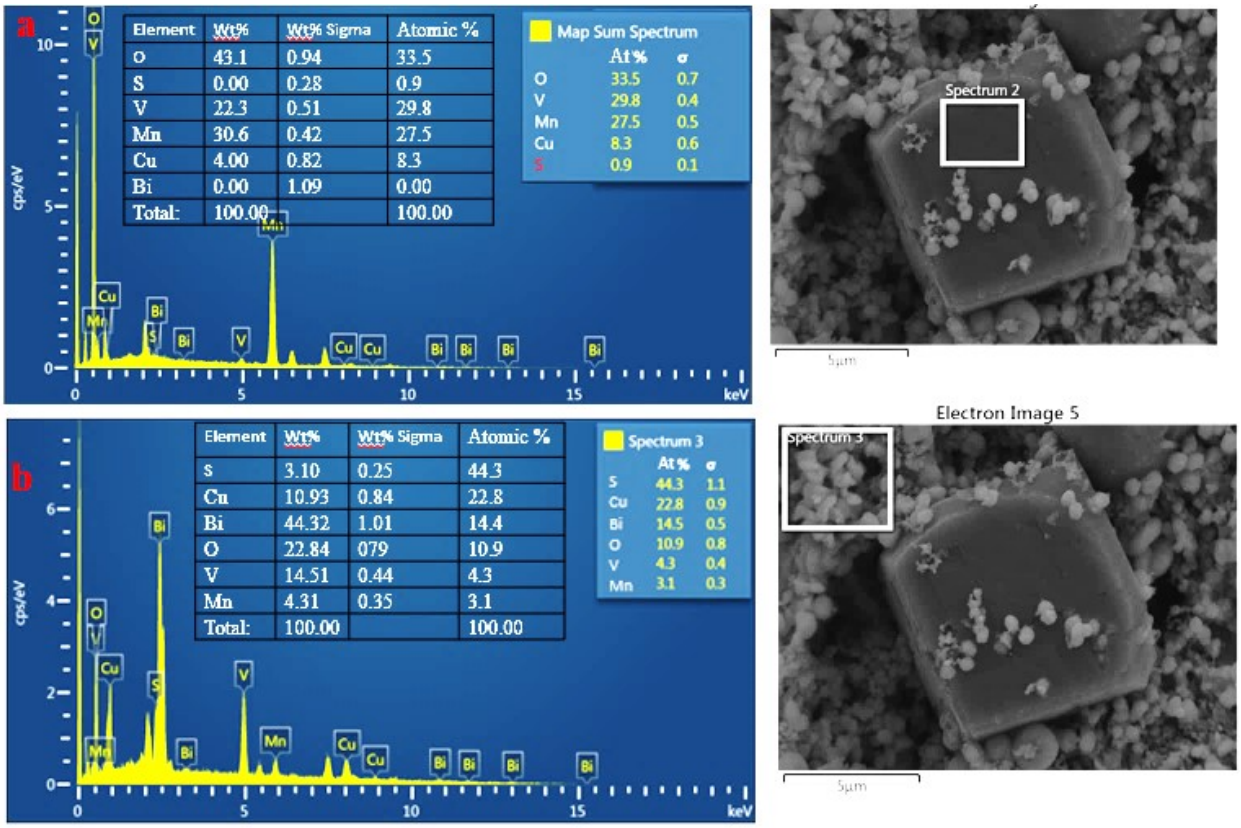

Fig. S2. (a, b) Small-area SEM-EDS spectra and composition analyses for individual (a) $Mn_4V_2O_9$ and (b) $Cu_4Bi_5S_{10}$ of the VCuMnBi(2:3:2:2) catalyst.

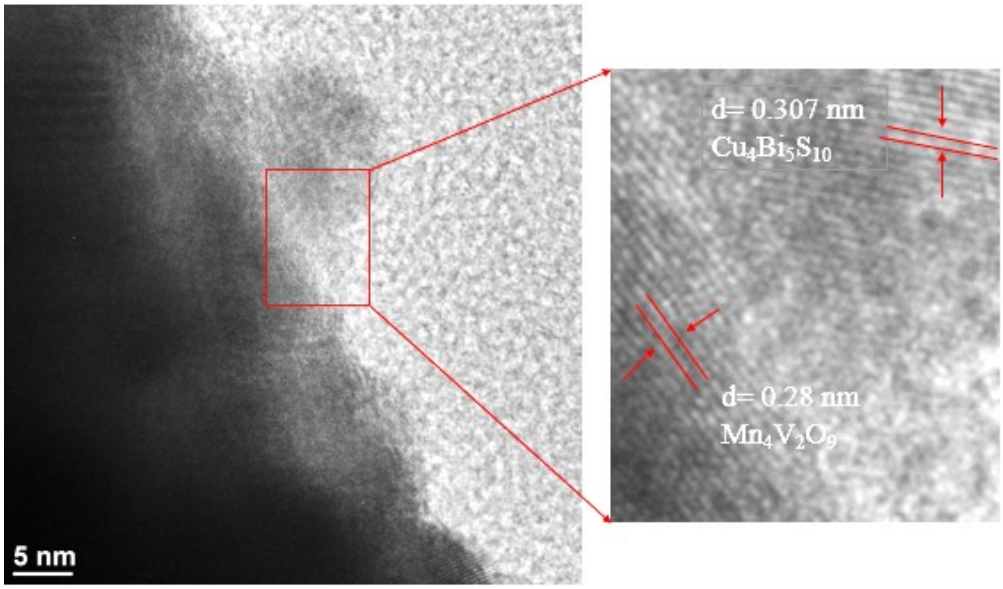

Fig. S3. The interface between $Cu_4Bi_5S_{10}$ and $Mn_4V_2O_9$.

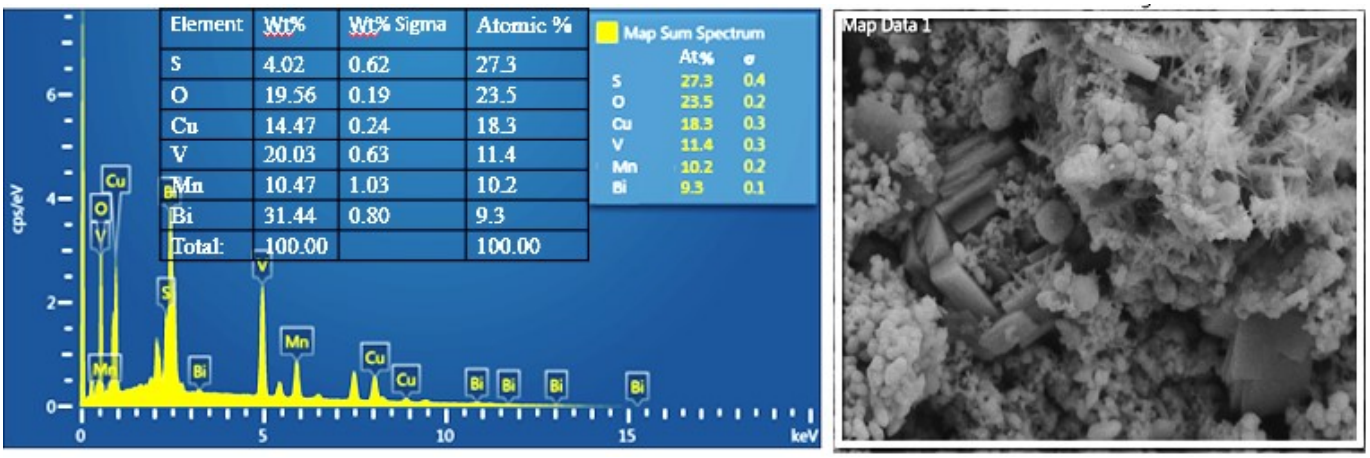

Fig. S4. SEM-EDS spectrum and the composition analysis, with contributions from the $Cu_4Bi_5S_{10}$ and $Mn_4V_2O_9$ phases shown in the SEM image.

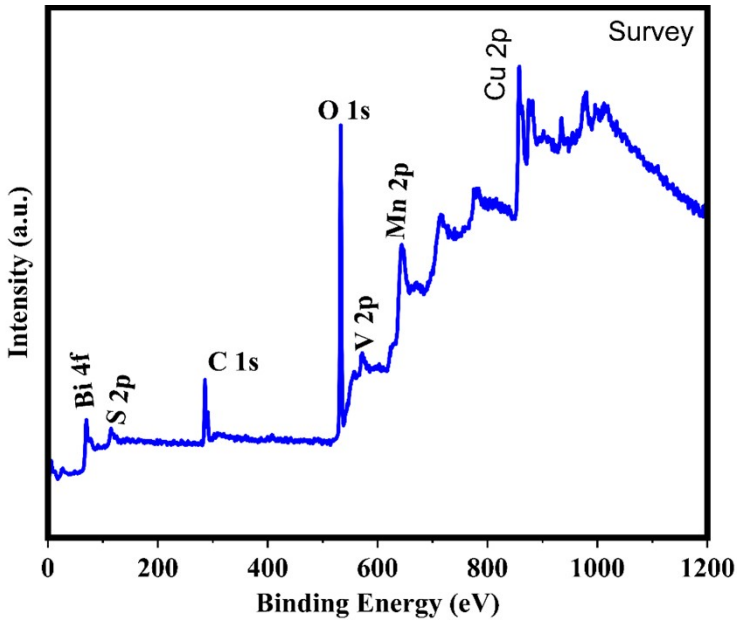

Fig. S5. XPS survey spectrum of the VCuMnBi(2:3:2:2) catalyst to show each element.

Table S2. XPS composition analyses for $Cu_4Bi_5S_{10}/Mn_4V_2O_9$ obtained from the VCuMnBi(2:3:2:2) system

Catalyst	Elements	Peak area (at.%)		
$Cu_4Bi_5S_{10}/Mn_4V_2O_9$	Cu	18.3	Cu^{+}	100
	S	27.3	S^{2-}	100
	V	11.4	V^{4+}	40.9
			V^{5+}	59.1
	Bi	9.3	Bi^{3+}	62.9
			Bi^{5+}	37.1
	Mn	10.3	Mn^{2+}	31.4
			Mn^{3+}	42.8
			Mn^{4+}	25.8
	O	23.5	O_L	41.1
			O_v	35.3
			O_{OH}	23.6

Table S3. Calculation of elemental compositions by the SEM-EDS data of $Cu_4Bi_5S_{10}/Mn_4V_2O_9$ obtained from the VCuMnBi(2:3:2:2) system

EDS from wide area	Cu	Bi	S	V	Mn	O
Molar ratio	18.3	9.3	27.3	11.4	10.2	23.5
$Mn_4V_2O_9$	0	For the cubic crystals, Mn and V valence states and the data from the bulk $Mn_4V_2O_9$ crystal with the basis of valence charge balance for cations and anions for an ionic compound, the $Mn_4V_2O_9$. phase can be viewed as $(Mn^{2+}_{0.312}Mn^{3+}_{0.429}Mn^{4+}_{0.259})_{10.2}(V^{4+}_{0.409}V^{5+}_{0.591})_{11.4}O_{23.5}$ (41.2/9) $(Mn^{2+}_{0.312}Mn^{3+}_{0.429}Mn^{4+}_{0.259})_{2.23}(V^{4+}_{0.409}V^{5+}_{0.591})_{2.49}(O^{2-}_{L})_{5.13}$ $\rightarrow(Mn^{2+}_{0.312}Mn^{3+}_{0.429}Mn^{4+}_{0.259})_{2.23}(V^{4+}_{0.409}V^{5+}_{0.591})_{2.49}(O_{9-3.87}^{2-})$ $\rightarrow(Mn^{2+}_{0.7}Mn^{3+}_{0.96}Mn^{4+}_{0.58}V^{4+}_{0.49}\square_{1.27})(V^{4+}_{0.53}V^{5+}_{1.47})_1(O_{9-y}^{2-})$ $\rightarrow(Mn^{2+}_{0.174}Mn^{3+}_{0.24}Mn^{4+}_{0.145}V^{4+}_{0.123}\square_{0.318})_4(V^{4+}_{0.265}V^{5+}_{0.735})_2O_{9-y}^{2-}$ $\rightarrow$4.58 $(Mn^{2+}_{0.174}Mn^{3+}_{0.24}Mn^{4+}_{0.145}V^{4+}_{0.123})_{4-0.318}(V^{4+}_{0.409}V^{5+}_{0.591})_2O_{9-y}^{2-}$ or 4.58 $(Mn,V)_{4-x}V_2O_{9-y}$ with 3.97/9= 43% oxygen vacancies and 0.318/4 ~ 8% Mn^{2+} vacancies				
	Theoretical	$Mn_4V_2O_9 = Mn^{2+}_4 V^{5+}_2 O_9$				
	⊕ Defects	Oxygen vacancy ($\bar{V}_O^{2+}$); Mn^{3+}-to-Mn^{2+} defect (Mn^{1+}_{Mn}); Mn^{4+}-to-Mn^{2+} defect (Mn^{2+}_{Mn}); V^{4+}-to-Mn^{2+} defect (V^{2+}_{Mn});				
	⊖ Defects	Mn^{2+} vacancy ($\bar{V}_{Mn}^{2-}$); V^{4+}-to-V^{5+} defect (V^{1-}_V);				
	4.58 × $(Mn,V)_{4-x}V_2O_{9-y}$					
$Cu_4Bi_5S_{10}$	18.3	For the snow like crystals, the components have 18.3% Cu and 9.3% Bi, where it has 62.9% Bi^{3+} and 37.01% Bi^{5+}. The $Cu_4Bi_5S_{10}$ phase can be viewed $Cu^{1+}_{18.3}(Bi^{3+}_{0.629}Bi^{5+}_{0.371})_{9.3}S_{26.6}$ (The 26.6 is close to the measured value, i.e. All S atoms were used for this compound. From Fig. S3, the slightly deficient anion sites can provide from O atoms.) $Cu^{1+}_{18.3}(Bi^{3+}_{0.629}Bi^{5+}_{0.371})_{9.3}(O^{2-}_{4.0}S^{2-}_{26.6})$ (30.6/10) x $Cu^{1+}_{5.98}(Bi^{3+}_{0.629}Bi^{5+}_{0.371})_{3.02}(O,S)_{10}$ 3.06 × $Cu^{1+}_{4.0}(Cu^{1+}_{1.98}Bi^{3+}_{1.90}Bi^{5+}_{1.12})S_{10}$ 3.06 × $Cu^{1+}_{4.0}(Cu^{1+}_{0.396}Bi^{3+}_{0.38}Bi^{5+}_{0.224})_5S_{10}$				

	Theoretical	$Cu_4Bi_5S_{10} = (Cu^{1+}_{0.5}Cu^{2+}_{0.5})_4(Bi^{3+}_{0.8}Bi^{2+}_{0.2})_5S_{10}$
	⊕ Defects	Bi^{5+}-to-Bi^{3+} defect (Bi^{2+}_{Bi}); Bi^{5+}-to-Bi^{2+} defect (Bi^{3+}_{Bi});
	⊖ Defects	Cu^{1+}-to-Cu^{2+} defect (Cu^{1-}_{Cu}); Cu^{1+}-to-Bi^{3+} antisite defect (Cu^{2-}_{Bi});
	3.06 × $Cu_4(Bi,Cu)_5S_{10}$	
	40 mol.% $Cu_4(Bi,Cu)_5S_{10}$ + 60 mol.% $Mn_{1-x}VO_{3-y}$	

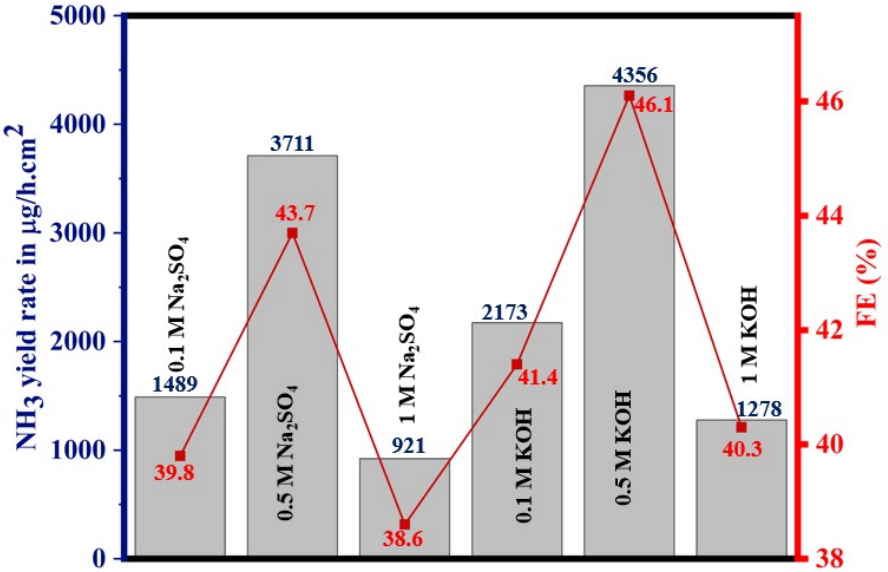

Fig. S6. eNRR yields at different KOH/Na_2SO_4-electrolyte concentrations.

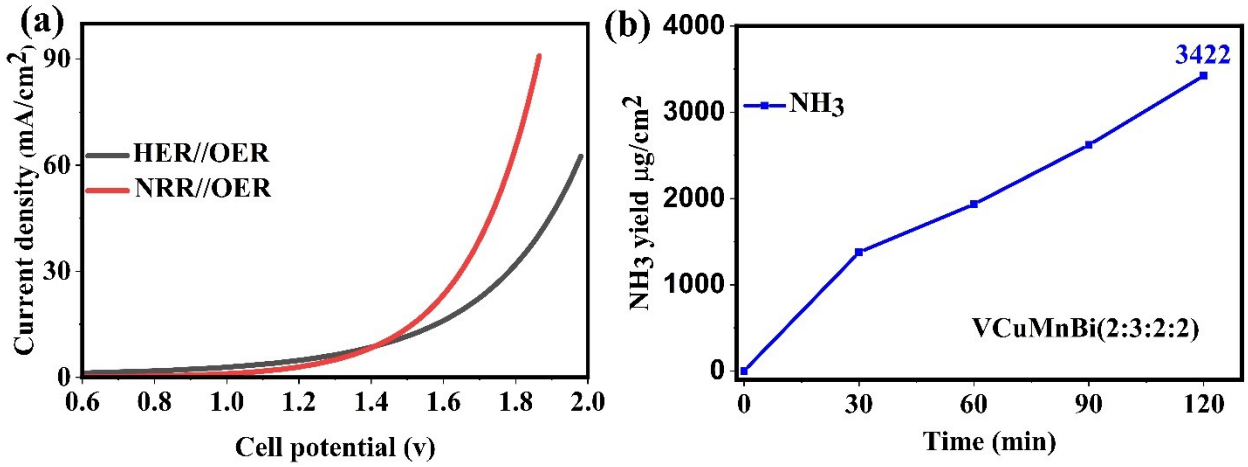

Fig. S7. (a) LSV curve and (b) eNRR production yields using a PEM flow stack cell system.

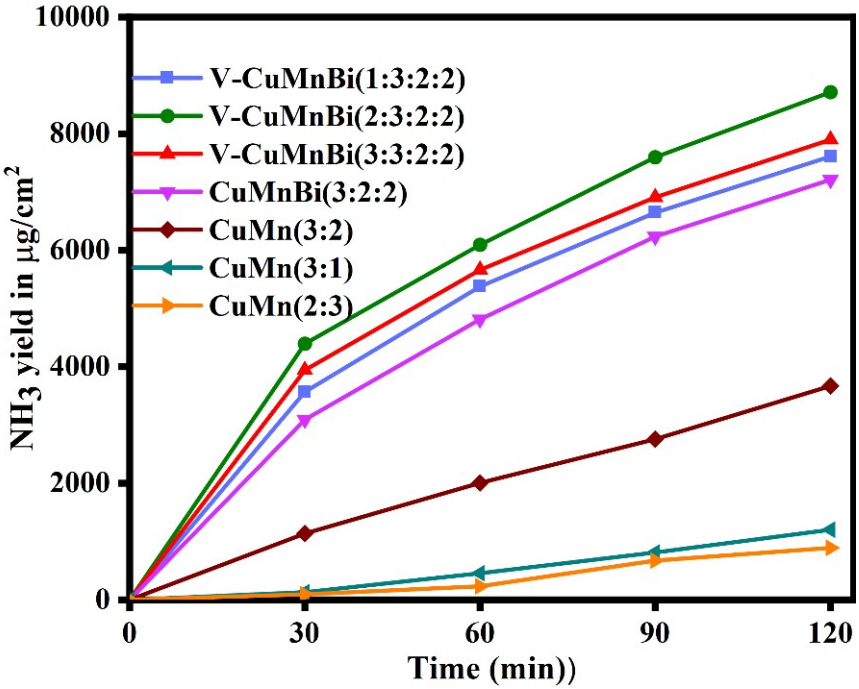

Fig. S8. eNRR ammonia yield *vs.* the reaction duration for different catalysts tested by Nessler's reagents.

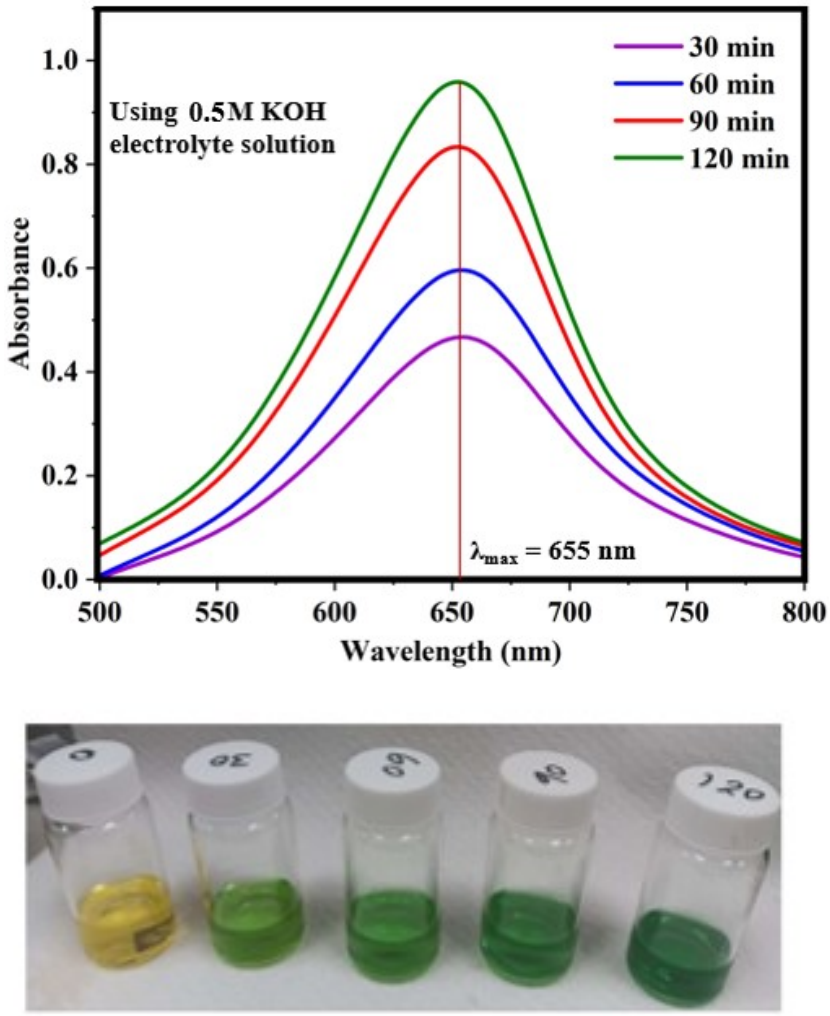

Fig. S9. UV-vis absorption spectroscopy for eNRR NH_3 for the VCuMnBi(2:3:2:2) catalyst to show the colors every 30 min after being tested by the IPB method.

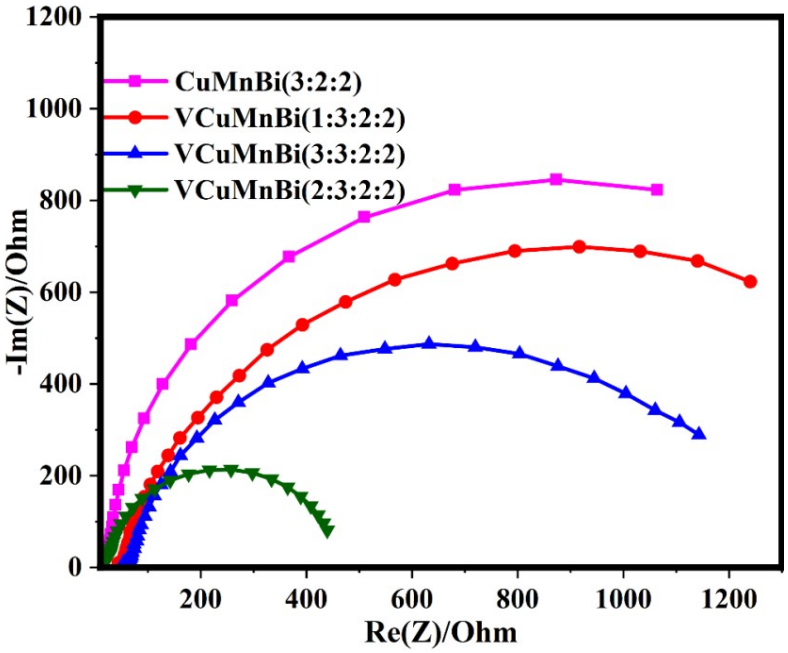

Fig. S10. EIS of various catalysts.

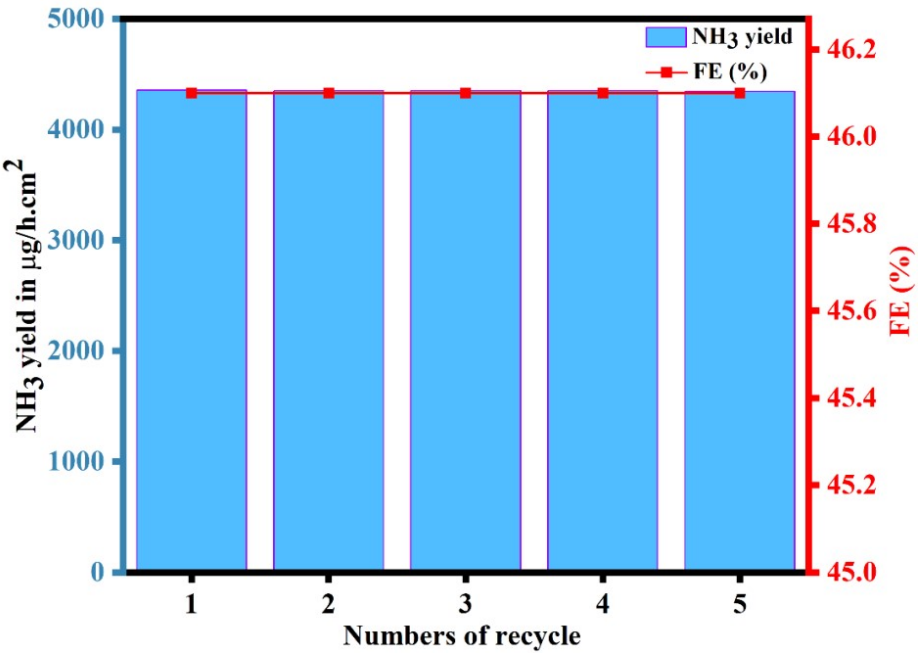

Fig. S11. Reusability test data of the leading catalyst.

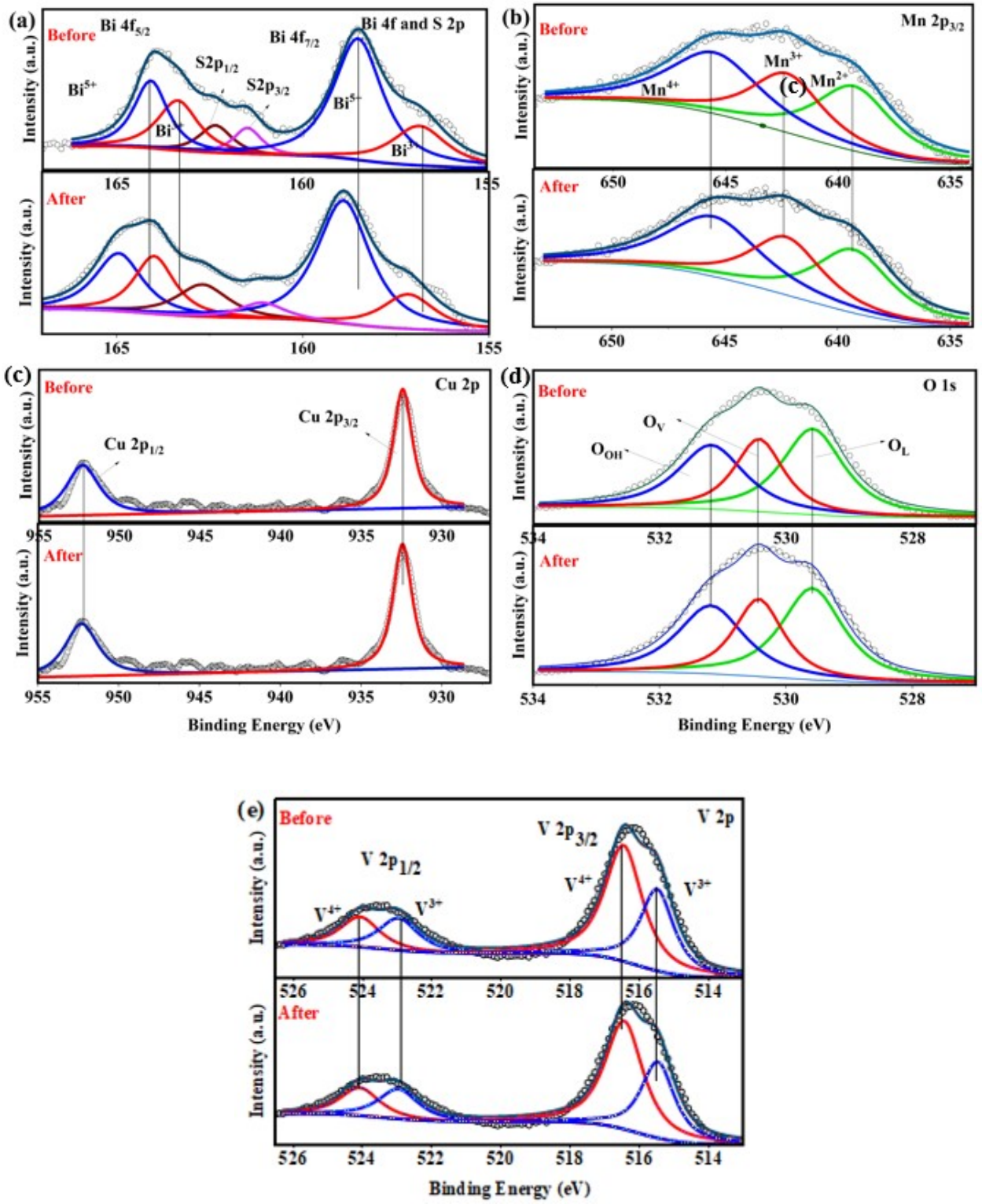

Fig. S12. XPS data of VCuMnBi(2:3:2:2) before and after the 12 h eNRR.

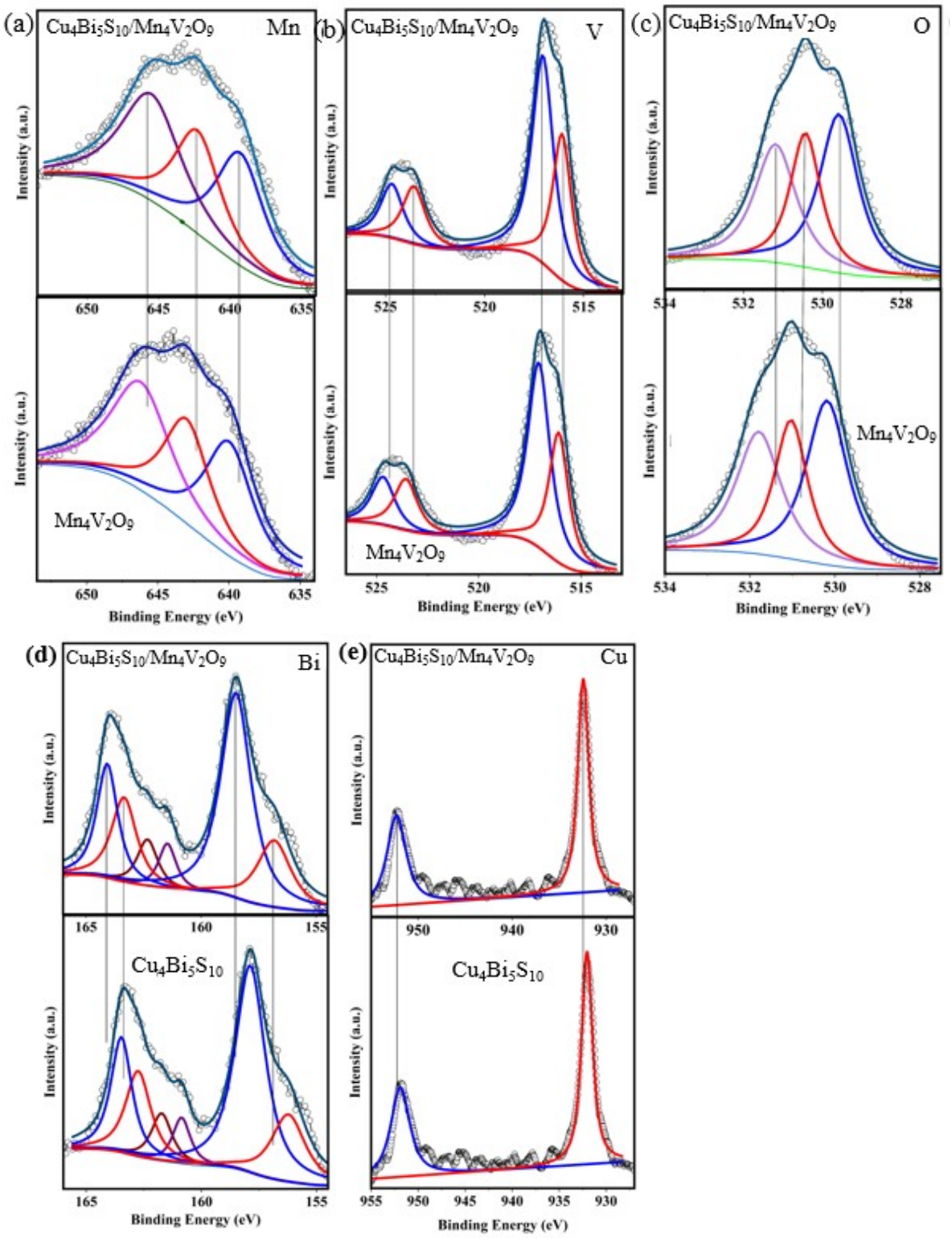

Fig. S13. XPS data of $Cu_4Bi_5S_{10}/Mn_4V_2O_9$ comparing with single $Mn_4V_2O_9$ or $Cu_4Bi_5S_{10}$ phase, produced by a binary metal hydrothermal reaction.

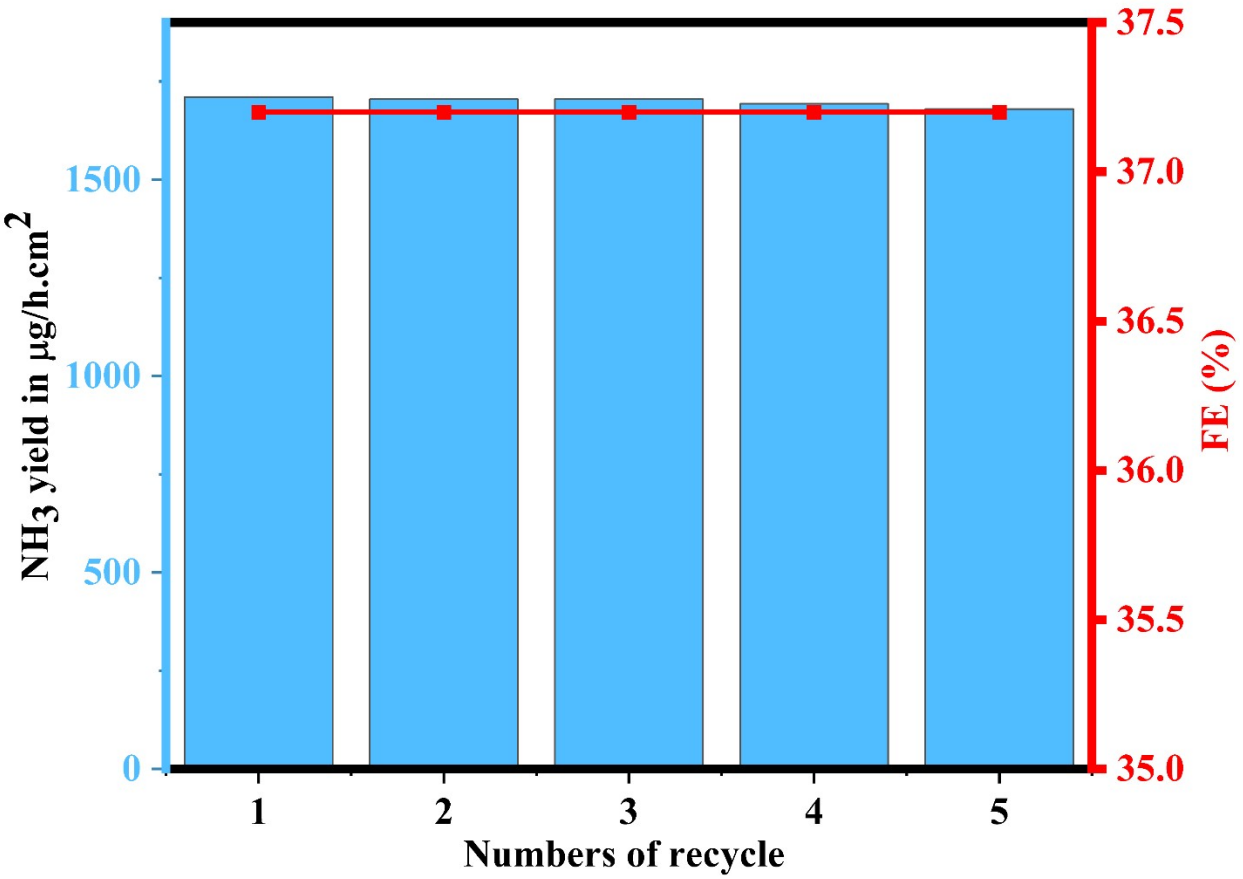

Fig. S14. Five times reusability test using leading catalyst by flow cell system.